Flow in a Channel with a Second-Order Fluid Under Transverse Flow Conditions

Mustapha Lamine[1], *Jamila Bouchgl*[2,3] and *Ahmed Hifdi*[1]

[1] Laboratory of Mechanics and High Energy Physics, Faculty of Sciences Aïn-Chock, Hassan II University of Casablanca, P.O. Box 5366 Maarif Casablanca 20100, Morocco.
[2] Higher Institute of Marine Fisheries-Agadir
[3] Laboratory of energy Engineering, Materials and Systems, ENSA, Ibn Zoher University, Agadir Morocco

Abstract. We examine the linear stability of a second-order fluid flow between two parallel, porous plates, with uniform transverse flow. An analytical approach was developed to obtain the base solution for stationary flows of a slightly viscoelastic fluid, which was then perturbed around the equilibrium state. The governing problem is formulated as a modified Orr–Sommerfeld equation and solved numerically using the Chebyshev collocation technique. Our numerical code was validated by reproducing classical results for a Newtonian fluid, with a critical Reynolds number Rec = 5772.22 and critical wave number α_c = 1.021 when transverse flow is absent. We then studied the influence of transverse injection, expressed by the injection Reynolds number R_c. For R_c = 0.2, 0.4, and 0.6, the flow shows increasing stabilization, with critical Reynolds numbers rising accordingly. When fluid elasticity is included, with K = -10^{-4}, the growth rate of the most unstable mode decreases by roughly 15%, delaying the onset of instability. At high R_c, elasticity and transverse flow combine to shift the flow to more stable regimes, highlighting how even slight viscoelasticity can significantly modify the transition to instability. These results provide a clearer understanding of how transverse flow and fluid elasticity interact to influence channel flow stability, with potential applications in polymer processing, filtration, and porous media flows.

1 Introduction

The stability of fluid flow in channel configurations has long been a subject of interest in fluid mechanics because of its importance in many practical applications, including heat transfer, filtration processes, polymer transport, and flows in porous structures. Predicting the transition from stable to unstable flow is essential for understanding transport mechanisms and improving the performance of engineering systems. For this reason, the effects of cross-flow, porous media [1,2], slip boundary conditions, and fluid properties on flow stability have been widely investigated.

Viscoelastic fluids, which exhibit both viscous and elastic behavior, can significantly alter flow characteristics compared to Newtonian fluids, particularly by influencing the onset of

instabilities. Although previous studies have examined the flow of Newtonian and some viscoelastic fluids, the understanding of the combined effects of transverse injection and fluid elasticity in porous channels remains limited.
The influence of uniform cross-flow and thermal effects on channel flow stability has been examined in several studies. Khan and Sani in [3] investigated the Poiseuille–Rayleigh–Bénard instability in a channel flow with uniform cross-flow and thermal slip, and showed that thermal boundary conditions play an important role in determining the stability limits. Shankar and Shivakumara [4] studied the hydrodynamic stability of plane porous-Couette flow with vertical throughflow and found that wall permeability significantly modifies the critical conditions for instability. The combined effects of porous media and slip boundary conditions were later analyzed by Badday and Harfash [5], who reported that both permeability and slip at the boundaries influence the behavior of Poiseuille flow.
More recent work has extended these investigations to complex fluid models. The authors in [6] showed that, viscoelastic effects can alter the onset of instability. Shivaraj Kumar and Basavaraj [7,8] examined the stability with uniform vertical cross-flow using different analytical approaches, providing further understanding of the mechanisms governing flow transition. The effect of more complex porous structures was considered by Hajool and Harfash [9], who studied instability in Poiseuille flow through a porous medium and highlighted the influence of the porous matrix on stability behavior.

The role of non-Newtonian fluid properties has also attracted considerable attention. A.S.Varghese and S. Panda [10] investigated the instability of a second-grade fluid and demonstrated the importance of fluid elasticity in modifying flow characteristics. In the context of viscoelastic fluids, Lamine et *al*. [11] carried out, in a plane channel, a linear stability analysis of flow and later examined the influence of uniform wall suction and blowing on the stability of a viscoelastic liquid [12]. Their results showed that elastic effects and wall mass transfer have a significant impact on the critical stability parameters.
Despite the progress achieved in these studies, the interaction between cross-flow, porous effects, slip conditions, and fluid elasticity is still not fully understood. A detailed analysis of these combined effects is necessary to improve the theoretical description of channel flow stability and to better understand transition mechanisms in complex fluids.

In this study, we take a different approach from that of previous studies to perform a linear stability analysis of flow with second-order fluid, between two porous and parallel plates. We highlight the effects of the transverse jet (at high flow rates) and the elastic properties of the fluid on the critical marginal stability threshold. This allows us to offer a new perspective on the stability of this flow.

2 Problem Formulation

We consider the Poiseuille flow, in the cartesian coordinate system (**x**, **y**), of a viscoelastic fluid between two parallel and porous plates. The plates are separated by $2d$ and extending infinitely in the **x** direction. A uniform transverse injection with velocity $v_0 = C^{te}$ is applied at **y**= +d corresponding to the upper wall, while suction *occurs* at the same velocity v_0 at $\boldsymbol{y} = -d$ corresponding to the lower wall.
The equations modelling the problem are:

$$\rho\left(\frac{\partial \boldsymbol{V}^*}{\partial t} + \boldsymbol{V}^*.\boldsymbol{\nabla}\boldsymbol{V}^*\right) = -\boldsymbol{\nabla}P^* + \boldsymbol{\nabla}\boldsymbol{\tau}^* \quad (1)$$

$$div\,\mathbf{V}^* = 0 \quad (2)$$

$\boldsymbol{V}^*$ represent the velocity field and P^* is the pressure. $\boldsymbol{\tau}^*$ is the stress tensor, defined for a second-order fluid:

$$\boldsymbol{\tau}^* = \mu\mathbf{A}_1 + \alpha_1\mathbf{A}_2 + \alpha_2\mathbf{A}_1^2 \;;\quad \alpha_1 < 0 \; et \; \alpha_2 \leq 0 \tag{3}$$

with

$$\mathbf{A}_1 = \nabla\mathbf{V}^* + (\nabla\mathbf{V}^*)^T \tag{4}$$

$$\mathbf{A}_2 = \frac{\partial\mathbf{A}_1}{\partial t^*} + (\mathbf{V}^*.\nabla\mathbf{A}_1) + \mathbf{A}_1.\nabla\mathbf{V}^* + (\nabla\mathbf{V}^*)^T.\mathbf{A}_1 \tag{5}$$

the strain rate tensors are $\boldsymbol{A}_1$ and $\boldsymbol{A}_2$, μ represent the dynamic viscosity, α_1 represents the viscosity jump and α_2 indicates the elasticity of the fluid.

2.1 Base flow solutions

Taking into account the translational invariance of the velocity in the longitudinal direction, the velocity field in the continuity equation simplifies in the equilibrium state to:

$$V^* = \left(U^*(y^*), v_o, 0\right) \tag{6}$$

with:

$$U^*(y^* = \pm d) = 0 \tag{7}$$

Substituting equations (3)–(6) into (1), corresponding to the Navier-Stokes equations, leads to the equation that governs the fluid's motion in the equilibrium state:

$$KR_c d\frac{\partial^3 U^*}{\partial y^{*3}} - \frac{\partial^2 U^*}{\partial y^{*2}} - \frac{R_c}{d}\frac{\partial^2 U^*}{\partial y^*} = \frac{\partial P^*}{\partial x^*} \tag{8}$$

Where $K = \frac{\alpha_2}{\rho d^2}$ and $R_c = \frac{\rho\, v_0 d}{\mu}$ represent the elasticity number and the Reynolds number of injection, respectively. For solving the problem in this case, given by equation (8), requires three boundary conditions. To close the problem, in addition to the two boundary conditions (7), an approximation is made regarding the nature of the fluid by assuming it is slightly viscoelastic [4], i.e., the elasticity number is small compared to unity. Using this approach, equation (8) becomes:

$$-\frac{\partial^2 U^*}{\partial y^{*2}} - \frac{R_c}{d}\frac{\partial U^*}{\partial y^*} = \frac{\partial P^*}{\partial x^*} \tag{9}$$

Using the reference quantities: d for length, $\frac{d}{U^*_{\max}}$ for time, $U^*_{\max}$ for velocity and $\rho U^{*2}_{\max}$ for pressure as follows:

$$y = \frac{y^*}{d}, x = \frac{x^*}{d}, t = \frac{U^*_{max}\, t^*}{d}, V = \frac{V^*}{U^*_{max}} = \left(\frac{U^*}{U^*_{max}}, \frac{v_0}{U^*_{max}}\right), P = \frac{P^*}{\rho(U^*_{max})^2}$$

The solution of the problem (9) in dimensionless variables is:

$$U(y) = R_c \frac{y + sinh^{-1}(R_c) - e^{-R_c y} - \coth(R_c)}{1 - \log\left(R_c^{-1} sinh(R_c)\right) - R_c \coth(R_c)} \tag{10}$$

In the case of $R_c \to 0$, corresponding to a transverse flow, we recover the classic form of the Poiseuille profile corresponding to (1-y^2).

2.2 Linear Stability Analysis

Two-dimensional infinitesimal disturbances (v, p) are superimposed on the equilibrium flow. Then, the solutions are sought in normal modes as follows using the theorem of Squire:

$$(v,p) = [\varphi(y), P']e^{i(\alpha x - \alpha ct)}\ ;\quad i^2 = -1 \qquad (11)$$

Where c is the propagation velocity, α is the wave number in the x-direction, φ and p' are the complex amplitudes of the stream function $\psi(x, y, t)$ and the disturbance p', respectively. This leads us to establish a differential equation that determines the stability of this flow, expressed as:

$$i\alpha \,\mathrm{Re}\left[(U-c)(D^2-\alpha)^2 - D^2U\right]\varphi - (D^2-\alpha^2)^2\varphi =$$
$$Rc(D^3 - \alpha^2 D^1)\varphi + i\alpha \,\mathrm{Re}\,K\left[(U-c)(D^2-\alpha)^2 - D^4U\right]\varphi \qquad (12)$$

In the case where R_c = 0, the second term of equation (12) accounts for the effect of elasticity, K. The boundary conditions associated with this equation are as follows:

$$\varphi(\pm 1) = D^1\varphi(\pm 1) = 0,\ avec\quad D^j = \frac{\partial^j}{\partial y^j}\quad j = 1,2,3,4 \qquad (13)$$

2.2.1 Numerical Method

Using the Chebyshev spectral collocation method [11], the equations (12) and (13) are solved numerically. In this approach, discretizing our system (12) and (13) at the Gauss-Lobatto collocation points (N) reduces the problem to a system below with eigenvalues c:

$$\mathbf{E}\varphi = c\mathbf{F}\varphi \qquad (14)$$

Note that **E** and **F** denote the matrices dependent on α, K, R_c and Re. Furthermore, to validate our computational code, we first verify the results obtained for a Newtonian fluid in the literature. In the second step, we check the results for a non-Newtonian fluid in the previous studies. For K=0 (Newtonian fluid), and without transverse flow, R_c=0: we compute the 32 least stable even and odd eigenvalues for the fundamental mode ($\alpha = 1$, *Re*=10000). We found a good agreement between our results and those obtained previously. Additionally, we accurately determined the stability thresholds for the flow of a Newtonian fluid (R_c=0 et *K*=0): Re_c= 5772.221 et α_c=1.02056. In the presence of transverse flow ($R_c \neq 0$), we compared our results with those of Fransson and Alfredsson [3]. Table1 summarizes this validation.

Table 1: Critical stability thresholds when K=0.

	Our results		Results in [9]	
R_c	Re_c	α_c	Re_c	α_c
0	5772.221	1.0205	5772.22	1.0205
0,2	5966.799	1.0132	5967,01	1,0118
0,4	6607.263	0.9913	6607,4	0,9902
0,6	7902.204	0.9551	7902,5	0,9536

As shown in this table, the critical stability thresholds obtained in our computations are in excellent agreement with those reported in [9]. The absolute differences in the critical Reynolds numbers (Rec) and wave numbers (αc) are very small on the order of 0.001–0.3 for Re_c and 0.001–0.0015 for α_c highlighting the accuracy of our numerical method and the reliability of the results.

For $K\neq0$, corresponding to a non-Newtonian fluid, and without a transverse flow (R_c=0), our results are in a good agreement with those of the previous studies. This comparison is shown in Table 2.

Table 2: Critical stability thresholds when R_c=0.

	Our results		Previous studies	
K	Re_c	α_c	Re_c	α_c
0	5772.221	1.02056	5772	1.0195
-0.00001	5638.376	1.0267	5639	1.0240
-0.00005	5167.848	1.0501	5168	1.0475
-0.0001	4698.682	1.0770	4698	1.0750
-0.0002	4014.524	1.1250	4014	1.1215

In this study, we assume a slightly viscoelastic fluid (K << 1) to simplify the analysis and obtain a tractable analytical solution. This assumption is physically justified because, in many industrial applications such as polymer transport or flow through porous media, elastic effects are small but not negligible. The primary influence of elasticity on flow stability can thus be captured without introducing the full complexity of strongly viscoelastic behavior. Additionally, the boundary conditions chosen uniform injection at the upper wall and uniform suction at the lower wall reflect practical situations where transverse flow can be controlled, such as in filtration or channelized flow systems. These conditions also facilitate the analytical and numerical treatment of the problem while preserving the main physical mechanisms governing the flow.

3 Results and Discussion

In the (Re_c, α_c) plane, the marginal stability curves for R_c = 0.2, 0.4 and 0.6, with the elasticity number fixed at K= - 10^{-5} and K= - 10^{-4}, are plotted in Figures 1 and 2, respectively. These curves indicate that increasing values of R_c are associated with a gradual stabilization of the flow. Therefore, the pair (Re_c, α_c) takes intermediate values between those observed when one of the control parameters (R_c et K) is present and the other is absent.
At specific values of Re_c = 6000 and α_c = 1, we qualitatively illustrate in Figure (3) the impact of increasing R_c on the amplitude of the imaginary part c_i of the most unstable eigenvalue, while fixing the elasticity number at K = 0, -10^{-5},-5.10^{-5},-10^{-4} et -2.10^{-4}.

From figure 3, we observe that when K=0, an increase in R_c causes the initially least stable mode to stabilize and then regain stability at higher values of R_c. The amplitude of the unstable mode increases with K for a given value of R_c *t*aking into account the elastic behavior of the fluid.

At large values of this parameter, elasticity reduces the amplitude of this unstable mode. Furthermore, the variation of R_c maintains the same shape of c_i as observed in the case of a

Newtonian fluid. However, the stabilization observed at high values of R_c is more prominent in the elastic fluid than in the Newtonian fluid.

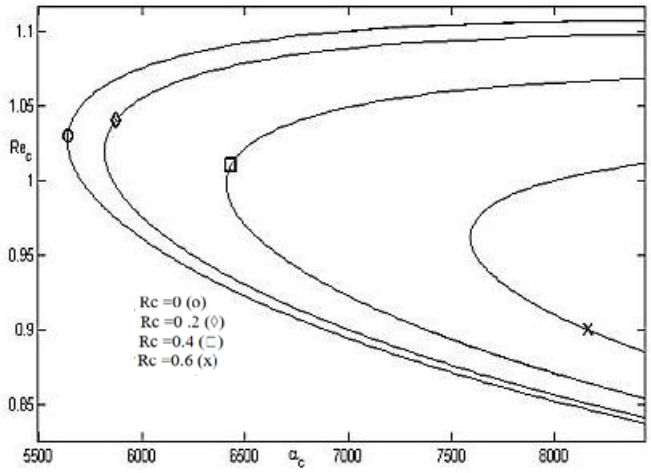

Fig. 1. Marginal stability curves at K=-10^{-5} [6] for different injection Reynolds number.

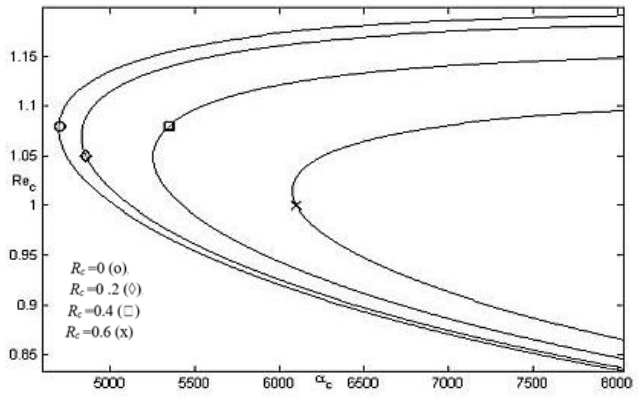

Fig. 2. Marginal stability curves at K=-10^{-4} [6] for different injection Reynolds number.

The table 3 bellow shows how the elasticity of the fluid (K) and the transverse flow (Rc) influence the stability of the channel flow. When the fluid becomes more elastic (K more negative), the critical Reynolds number decreases, meaning the flow becomes unstable more easily. When a transverse flow is applied (Rc > 0), the critical Reynolds number increases, indicating that the flow is more stable. This gives a clear, quantitative view of the effects of these two parameters on flow stability.

The observed trends show that increasing the transverse injection Rc stabilizes the flow by suppressing the growth of the least stable modes, while increasing fluid elasticity K tends to either stabilize or destabilize the flow depending on its magnitude. Specifically, for small negative values of K, the amplitude of the most unstable mode decreases, delaying the onset of instability, whereas at higher elasticity, the interaction with Rc produces more complex behavior. This analysis links the numerical results directly to the physical

processes governing the flow, providing a more robust qualitative and quantitative understanding of the system.

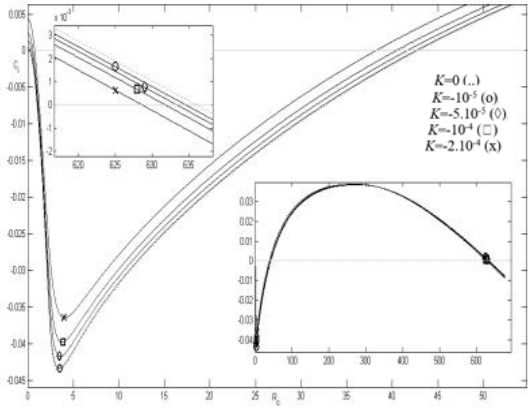

Fig. 3. Effect of R on the imaginary part of the largest eigenvalue of the fundamental mode (Re_c =6000; α_c=1), for different values of K.

Table 3: Combined effect of K and Rc on the critical stability threshold
(Re_c = 5772.22; α_c = 1.02056)

R_c \ K	0	-10^{-5}	-5.10^{-5}	-10^{-4}	-2.10^{-4}	
0	5772.221	5638.37	5167.85	4698.68	4014.52	R_{ec}
	1.02056	1.0267	1.0501	1.0770	1.1250	α_c
0.2	5966.799	5824.32	5331.28	4839.89	4126.96	R_{ec}
	1.01320	1.0194	1.0428	1.0697	1.1174	α_c
0.4	6607.263	6438.22	5854.85	5282.52	4465.76	Rec
	0.99130	0.9976	1.0214	1.0485	1.0961	α_c
0.6	7902.204	7671.76	6890.68	6144.42	5110.64	R_{ec}
	0.95510	0.9617	0.9864	1.0141	1.0623	α_c

Our results are consistent with recent literature on viscoelastic and second-order fluid flows in channels. For instance, Shankar & Shivakumara [13] studied the linear stability of plane channel flow of a Navier–Stokes–Voigt fluid with vertical through flow and identified complex neutral stability curves and coupled effects of throughflow and viscoelasticity on the onset of instability [6]. Their findings highlight that the interaction of through flow and viscoelasticity can lead to non-trivial stability characteristics, which complements our observation that transverse flow (Rc) and fluid elasticity (K) interact to delay or promote instability depending on the parameter range. Similarly, Lamine et *al.* [11] demonstrated the influence of fluid elasticity on channel flow stability, further confirming the relevance of elastic effects in stabilizing or destabilizing flows.

4 Conclusion

This study analyzed the linear stability of a second-order fluid flowing between two parallel, porous plates with a uniform transverse flow. For a Newtonian fluid without transverse flow, the critical Reynolds number was found to be 5772.22 with a critical wave number of 1.021. Introducing transverse flow increased the critical Reynolds number, reaching 5966.8, 6607.3, and 7902.2 for Rc = 0.2, 0.4, and 0.6, showing that cross-flow stabilizes the system. When fluid elasticity was included ($K = -10^{-4}$), the growth rate of the most unstable mode decreased by about 15%, delaying the onset of instability. At high transverse flow rates, elasticity and cross-flow combined to further stabilize the flow, demonstrating that even slight viscoelasticity can significantly influence flow behavior.

Although this study is primarily numerical, the results provide useful quantitative insights for practical applications such as polymer transport, filtration, and heat transfer. In particular, the stabilizing effects of transverse flow and fluid elasticity on the critical stability thresholds could inform the design and optimization of systems involving slightly viscoelastic fluids. Future work could focus on translating these numerical findings into concrete engineering guidelines.

Overall, these results quantify how transverse injection and fluid elasticity interact, offering valuable perspectives for fluid handling, industrial processes, and flows in porous media.

References

[1] M. Assoul, A. El jaouahiry, J. Bouchgl, M. Echchadli, S. Aniss, Effect of Horizontal Quasi-Periodic Oscillation on the Interfacial Instability of Two Superimposed Viscous Fluid Layers in a Vertical Hele-Shaw Cell, Fluids, 8, 6 (2023). https://doi.org/10.3390/fluids8060164.

[2] J. Bouchgl, S. Aniss, S., Effect of periodic oscillation on the interfacial instability of two superposed fluid layers in a fully saturated porous media, Int. J. Appl. Mech., **13**, 2150088 (2021). https://doi.org/10.1142/S1758825121500885

[3] MBM. Khan, M. Sani, S. Ghosh, H. Behera, Poiseuille-Rayleigh-Benard instability of a channel flow with uniform cross-flow and thermal slip, Phys. Fluids, **33**, 053612 (2021). https://doi.org/10.1063/5.0050006.

[4] B.M. Shankar, I.S. Shivakumara, Changes in the hydrodynamic stability of plane porous-Couette flow due to vertical through flow, Phys. Fluids, **33**, 074103 (2021). https://doi.org/10.1063/5.0054179.

[5] A.J. Badday , A.J. Harfash, Instability in Poiseuille flow in a porous medium with slip boundary conditions and uniform vertical throughflow effects, J. Eng. Math., **135**, 6, (2022). https://doi.org/10.1007/s10665-022-10231-w

[6] B.M. Shankar, I.S. Shivakumara, Stability of plane Poiseuille and Couette flows of Navier-Stokes-Voigt fluid, Acta. Mech., **234**, 4589 (2023). https://doi.org/10.21203/rs.3.rs-2497965/v1

[7] D.L. Shivaraj Kumar , M.S. Basavaraj , Dual analysis of stability in plane Poiseuille channel flow with uniform vertical cross flow, Phys. Fluids, **36**, 034106 (2024). https://doi.org/10.1063/5.0191925

[8] D.L. Shivaraj Kumar , M.S. Basavaraj, Stability patterns in plane porous Poiseuille flow with uniform vertical cross-flow: a dual approach, Int. J. Non-Linear Mech., **165**, 104797 (2024).

https://doi.org/10.1016/j.ijnonlinmec.2024.104797

[9] S.S. Hajool, A.J. Harfash, Instability of Poiseuille flow in a bidisperse porous medium subject to a uniform vertical through flow effect, ASME J. Fluids Eng., **146**, 051301 (2024). https://doi.org/10.1115/1.4064102.

[10] A.S. Varghese , S. Panda, Flow instabilities of second-grade fluid over a stretching sheet, Eur. J. Mech. B/Fluids, **102**, 135 (2023). https://doi.org/10.1016/j.euromechflu.2023.07.009

[11] M. Lamine, S. Aniss, A. Hifdi, Linear Stability Analysis of Viscoelastic Fluids in a Plane Channel Flow, Advances in Mechanics. CMM 2022. Lecture Notes in Mechanical Engineering. Springer, Cham, (2024). https://doi.org/10.1007/978-3-031-46973-2_12

[12] M. Lamine, A. Hifdi, Stability analysis of a viscoelastic liquid in a channel flow with uniform wall suction/blowing, J. Eng. Math., **152**,1 (2025). https://doi.org/10.1007/s10665-025-10463-6.

[13] B.M.Shankar, Shivakumara I.S, On the hydrodynamic stability of channel flow of a Navier–Stokes–Voigt fluid with vertical throughflow, Int. J. of Non-Linear Mech., **178**, (2025). https://doi.org/10.1016/j.ijnonlinmec.2025.105224.